

Thermo-optic effect and optical third order nonlinearity in nc-Si embedded in a silicon-nitride film

C. Torres-Torres^{1*}, A. López-Suárez², L. Tamayo-Rivera³, R. Rangel-Rojo³, A. Crespo-Sosa², J. C. Alonso⁴, and A. Oliver²

¹Sección de Estudios de Posgrado e Investigación-ESIME-IPN, Zacatenco, México, D.F., 07738, México

²Instituto de Física, Universidad Nacional Autónoma de México, A.P. 20-364, México, D. F. 01000, México.

³CICESE/División de Física Aplicada, A.P. 360, Ensenada, B.C. 22860 México

⁴Instituto de Investigaciones en Materiales. Universidad Nacional Autónoma de México, A.P. 70-360, México, D. F. 04510, México.

*Corresponding author: crstorres@yahoo.com.mx

Abstract: Using a self-diffraction experiment with 7ns pulses at 532nm we studied a silicon nitride film containing silicon nanoclusters (nc-Si) of 3.1 ± 0.37 nm mean size. The sample was prepared by remote plasma-enhanced chemical vapor deposition (RPECVD), and we found that its nonlinearity consists of a combination of electronic and thermal contributions. By varying the repetition rate of the laser, we discriminated the responsible mechanisms for the nonlinear response. Using this procedure we determined a total $|\chi_{1111}^{(3)}| = 3.3 \times 10^{-10}$ esu, $n_2 = 2.7 \times 10^{-16}$ m²/W, $\beta = 1 \times 10^{-9}$ m/W and $dn/dT = 1 \times 10^{-4}$ °C⁻¹ for our sample. We also show results for the optical Kerr effect using 80 fs pulses at 820 nm. The purely electronic nonlinearity measured is characterized by $|\chi_{1111}^{(3)}| = 9.5 \times 10^{-11}$ esu.

©2008 Optical Society of America

OCIS codes: (160.4330) Nonlinear optical materials; (190.3270) Kerr effect; (160.6840) Thermo-optical materials.

References and links

1. L. Domash, M. Wu, N. Nemchuk, E. Ma, "Tunable and Switchable Multiple Cavity Thin Film Filters," *J. Lightwave Technol.* **22**, 126-135 (2004).
2. M. W. Pruessner, T. H. Stievater, M. S. Ferraro, W. S. Rabinovich, "Thermo-optic tuning and switching in SOI waveguide Fabry-Perot microcavities," *Opt. Express*, **15**, 7557-7563 (2007).
3. Y. Li, J. Yu, and S. Chen, "Rearrangeable nonblocking SOI waveguide thermo optic 4x4 switch matrix with low insertion loss and fast response," *IEEE Photon. Technol. Lett.* **17**, 1641-1643 (2005).
4. R. W. Boyd, *Nonlinear Optics*, (Academic Press, San Diego, 1992).
5. M. von Allmen and A. Blatter *Laser-beam interaction with materials*, (Berlin, Springer, 1995) Chap. 3.
6. C. Torres-Torres, A. V. Khomenko, J. C. Cheang-Wong, L. Rodríguez-Fernández, A. Crespo-Sosa, A. Oliver, "Absorptive and refractive nonlinearities by four-wave mixing for Au nanoparticles in ion-implanted silica," *Opt. Express*, **15**, 9248-9253 (2007).
7. G. Santana, B. M. Monroy, A. Ortiz. L. Huerta, J.C. Alonso, "Influence of the surrounding host in obtaining tunable and strong visible photoluminescence from silicon nanoparticles," *Appl. Phys. Lett.* **88**, 041916(1) - 041916(3) (2006).
8. T. Y. Kim, Nae-Man Park, Kyung-Hyun Kim, G. Y. Sung, Young-Woo Ok, Tae-Yeon Sung, Cheol-Jong Choi, "Quantum confinement effect of silicon nanocrystals in situ grown in silicon nitride films," *Appl. Phys. Lett.* **85**, 5355-5357 (2004).
9. A. Benami, G. Santana, A. Ortiz, A. Poce, D. Romeu, J. Aguilar-Hernández, G. Contreras-Puente, J. C. Alonso, "Strong white and blue photoluminescence from silicon nanocrystals in SiN_x grown by remote PECVD using SiCl₄/NH₃," *Nanotechnology* **18**, 155704-155709 (2007).
10. G. Heng-Qun and W. Qi-Ming, "Nonlinear optical response of nc-Si-SiO₂ films studied with femtosecond four-wave mixing technique," *Chin. Phys. Lett.* **23**, 2989-2992 (2006).
11. M. Dinu, F. Quochi, and H. Garcia, "Third-order nonlinearities in silicon at telecom wavelengths," *Appl. Phys. Lett.* **82**, 2954-2956 (2003).

12. P. Cheng, H. Zhu, Y. Bai, Y. Zhang, T. He, Y. Mo, "Third-order nonlinear optical response of silicon nanostructures dispersed in organic solvent under 1064 nm and 532 nm laser excitations," *Opt. Commun.*, **270**, 391-395 (2007).
13. I. Umezu, T. Yamaguchi, K. Kohno, M. Inada, and A. Sugimura, "Preparation of SiN_x film by pulsed laser ablation in nitrogen gas ambient," *Appl. Surf. Sci.* **197**, 376-378 (2002).
14. C. Torres-Torres, J. A. Reyes-Esqueda, J. C. Cheang-Wong, A. Crespo-Sosa, L. Rodríguez-Fernández, and A. Oliver, "Optical third order nonlinearity by nanosecond and picosecond pulses in Cu nanoparticles in ion-implanted silica," *J. of Appl. Phys.* **104**, 014306 (2008).

1. Introduction

The nonlinear optical properties of nanostructures have conducted to several studies due to their potential applications on optical communication networks. Filters, modulators or multiplexers for optical signals can be achieved by taking advantages of the nonlinear and thermal properties of thin film materials containing nanostructures [1-3]. An intense optical wave can modify, by means of the optical Kerr effect, the index of refraction in a material. This property has potential applications for all-optical devices and it can result from different physical mechanisms: fast responding ones such as electronic polarization, molecular orientation, or slow ones such as the thermal response arising from absorption [4]. In this work we investigate the optical nonlinearity of a silicon nitride film grown by RPECVD containing nc-Si. We also show a procedure by which the relative contribution of a slow thermal and a fast electronic mechanisms have in the total nonlinear response, based on a multiwave mixing experiment with nanosecond pulses. Thermal effect becomes important for relatively long pulses and when there is a significant amount of linear absorption. Our technique is based on a comparison of the vectorial self-diffracted intensities obtained when the repetition rate of the pulses is changed. As a comparative result we have also conducted a time-resolved femtosecond optical Kerr gate experiment for measuring the optical response in the regime of very short pulses, and far from resonance where we expect the nonlinearity to be purely an electronic polarization effect without important thermal contributions.

2. Theory of self-diffraction in a non-steady state of thermal diffusion

The relaxation of the change of density associated with a thermal effect induced by an optical wave in our sample can be estimated by calculating the temperature increment between pulses with the use of the heat equation presented in Ref. [5],

$$\frac{\partial T}{\partial t} = \frac{\partial}{\partial z} \left[\frac{\kappa}{\rho C} \frac{\partial T}{\partial z} \right] + \frac{\alpha}{\rho C} I(t, z), \quad (1)$$

here T is the temperature, which is a function of the depth z , κ is the thermal conductivity, ρ is the density, C the heat capacity, t is the pulse duration, α is the linear absorption coefficient and I the optical intensity. In order to identify the optical Kerr effect in a sample with length z , we consider the interaction of two coherent optical waves with wavelength λ . A grating of index, $\Psi_{\pm}(x)$, is generated by means of an optical Kerr effect, with $\Psi_{\pm}(x)$ given by:

$$\Psi_{\pm}(x) = \Psi_{\pm}^{(0)} + \Psi_{\pm}^{(1)} \cos \frac{2\pi x}{\Lambda}, \quad (2)$$

where

$$\Psi_{\pm}^{(0)} = \frac{4\pi^2 z}{\left(n_0 + \frac{dn}{dT} \Delta T\right) \lambda} \left[A \left(|E_{1\pm}|^2 + |E_{2\pm}|^2 \right) + (A + B) \left(|E_{1\mp}|^2 + |E_{2\mp}|^2 \right) \right], \quad (3)$$

$$\Psi_{\pm}^{(1)} = \frac{4\pi^2 z}{\left(n_0 + \frac{dn}{dT} \Delta T\right) \lambda} \left[A E_{1\pm} E_{2\pm}^* + (A + B) E_{1\mp} E_{2\mp}^* \right] + \frac{2\pi z}{\lambda} \frac{dn}{dT} \Delta T. \quad (4)$$

Here $K=2\pi/\Lambda$ is the wave number of the induced grating, $A = 6\chi_{1122}^{(3)}$ and $B = 6\chi_{1221}^{(3)}$, are the components of the third-order susceptibility tensor $\chi^{(3)}$ [4]. For long pulse interactions, or multishot irradiation, we can calculate the refractive index in Eqs. (3), (4) taking into account the thermo-optic coefficient, dn/dT , and the change in the temperature, ΔT . Consecutive laser pulses impinging on the sample will result in an accumulative index change. Self-diffracted intensities must change strongly as a function of dn/dT when interference fringes occur and a thermal Kerr effect is present. In agreement with a previous analysis made in Ref. [6], we can write the expressions for the zero and first order of diffraction equations generated in a nonlinear absorptive media interacting with two incident waves as:

$$E_{1\pm}(z) = \left[J_0(\Psi_{\pm}^{(1)})E_{1+}^0 + iJ_1(\Psi_{\pm}^{(1)})E_{2+}^0 \right] \exp\left(-i\Psi_{\pm}^{(0)} - \frac{\alpha(I)z}{2}\right), \quad (5)$$

$$E_{2\pm}(z) = \left[J_0(\Psi_{\pm}^{(1)})E_{2+}^0 - iJ_1(\Psi_{\pm}^{(1)})E_{1+}^0 \right] \exp\left(-i\Psi_{\pm}^{(0)} - \frac{\alpha(I)z}{2}\right), \quad (6)$$

$$E_{3\pm}(z) = \left[iJ_1(\Psi_{\pm}^{(1)})E_{1+}^0 - J_2(\Psi_{\pm}^{(1)})E_{2+}^0 \right] \exp\left(-i\Psi_{\pm}^{(0)} - \frac{\alpha(I)z}{2}\right), \quad (7)$$

$$E_{4\pm}(z) = \left[-iJ_1(\Psi_{\pm}^{(1)})E_{2+}^0 - J_2(\Psi_{\pm}^{(1)})E_{1+}^0 \right] \exp\left(-i\Psi_{\pm}^{(0)} - \frac{\alpha(I)z}{2}\right), \quad (8)$$

where $E_{1\pm}(z)$ and $E_{2\pm}(z)$ are the complex amplitudes of the circular components of the transmitted waves beams; $E_{3\pm}(z)$ and $E_{4\pm}(z)$ are the amplitudes of the self-diffracted waves, while E_{1+}^0 and E_{2+}^0 are the amplitudes of the incident waves; the irradiance dependent absorption coefficient $\alpha(I)=\alpha_0+\beta I$, where α_0 and β represent the linear and two-photon absorption coefficients, respectively, and $J_m(\Psi_{\pm}^{(1)})$ stands for the Bessel function of order m .

3. Experiment

The silicon-nitride film was prepared using a RPECVD system. The film was grown on a quartz substrate using a working pressure of 300 mTorr, a substrate temperature of 300°C, a power of 300 W and a time deposition of 20 min. The flow rates of H_2 , Ar, SiH_2Cl_2 and NH_3 were 20, 150, 5 and 50 sccm, respectively. The elemental composition of the film was obtained by Rutherford Backscattering Spectrometry (RBS) using the 3MV Tandem accelerator (NEC 9SDH-2 Pelletron) facility at the Instituto de Física of the Universidad Nacional Autónoma de México (UNAM). A collimated 3.045 MeV α -particle beam of 1.5 mm diameter was used as projectile. After the collision, the scattered alpha particles were detected with a surface barrier detector placed at 168°. We used a Xe lamp, 244 nm, as excitation source for the photoluminescence (PL) measurements and HRTEM images of our sample were obtained with a JEOL JEM-2010F FasTEM microscope operating at 200 kV with a GATAN digital micrograph system for image acquisition.

For the nanosecond self-diffraction experiment we used a Nd-YAG laser with 7ns pulses, 4mJ of energy, linear polarization, and $\lambda=532$ nm. The intensity rate of the incident beams was 1:1. The radius of the beam waist at the focus in the sample was measured to be 0.06 mm.

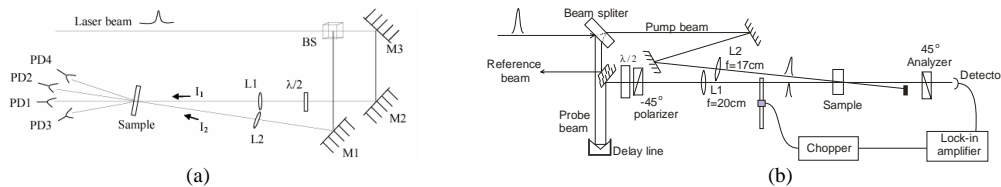


Fig. 1. Optical set up for (a) self-diffraction experiment, (b) Kerr gate experiment.

Figure 1(a) shows the optical experimental set up, where L1-2 represent the focusing system of lens, BS a beam splitter, $\lambda/2$ represent a half-wave plate, M1-3 are mirrors and PD1-4 are photodetectors with integrated filters. For measuring the optical Kerr response in absence of thermal effects, we used a Ti:sapphire laser with $\lambda=830$ nm, 80fs pulses, 3.4nJ maximum pulse energy and a repetition rate of 94MHz. Figure 1(b) shows the experimental set up for our Kerr gate experiment. A pump and probe beams, with an intensity relation of 10:1, and their linear polarizations making an angle of 45° are focused in the sample with a spot of $80\mu\text{m}$. The probe intensity is measured through an analyzer with its transmission axis crossed respect to the initial polarization of the probe beam. By delaying the probe beam with respect to the pump beam, we can observe a change in the transmittance of the system and measure the decay of the induced birefringence in the sample.

4. Results and discussion

RBS result showed the atomic percentage concentration of the film to be 62% Si, 26% N and 12% Cl. The film thickness, 703 ± 35 nm, was calculated using a profilometer system. The RBS spectrum did not show any oxygen presence in the film and our sample exhibits a good chemical stability. This stability is a consequence of the presence of hydrogen that comes from the NH_3 gas and that helps the silicon-nitride film to grow with low content of Cl in its network. If a large amount of Cl were incorporated into the sample, it would make the film network to become more open, so when the sample were uploaded from the deposition chamber and exposed to atmosphere, the oxygen and water vapor could diffuse into the film and create chemical unstable films. In Fig. 2 we show the PL signal and the linear optical absorption spectrum of our sample.

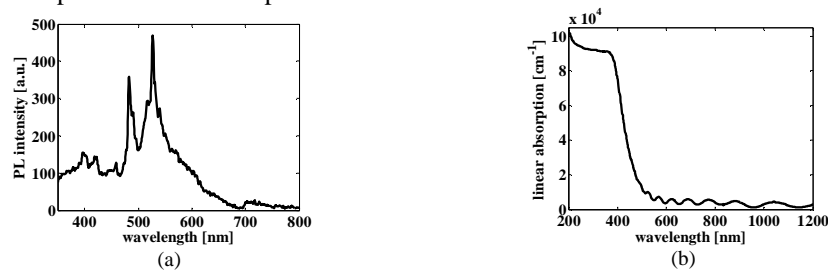


Fig. 2. (a) PL spectrum (b) Linear optical absorption spectrum.

The PL spectrum of the silicon nitride sample shows the signature of nc-Si formation[7]. According to the confinement model [8] the average size of the quantum dots of nanoclusters can be calculated using the relation $E_p(\text{eV}) = E_{\text{bulk}} + C_q/a^2 = 1.16 + 11.8/a^2$, where E_p is the measured PL energy peak, E_{bulk} is the band-gap energy of the bulk crystal silicon, C_q is the quantum confinement parameter and a is the average size (nm) of the nanocluster. The calculated average sizes of the nc-Si are 2.89 and 3.15 nm, corresponding to the peaks observed from Fig. 2(a) and located at 482 and 528 nm, respectively. The absorption spectrum in Fig. 2(b) shows a well defined absorption edge around 400 nm. The modulation observed for longer wavelengths is due to multi reflection interference effect in the thin film matrix of our sample [9]. Our sample behaves like a Fabry-Perot interferometer for transmitting and filtering optical wavelengths. We observed that the absorption peaks change uniformly their position in the spectrum when we modified slightly the incident angle of the light used for measuring the linear absorption. An important absorption is presented at 532nm but we can consider there is not a resonance response in this wavelength for our sample.

In Fig. 3(a) we showed a panoramic view of one region of the sample, where the nc-Si appear as dark rounded spots, while the silicon substrate appears as a lighter region surrounding the nanocrystals. A statistical analysis of HRTEM images showed that the size of nc-Si varied from 1.8 ± 0.21 to 4.1 ± 0.49 nm, with an average size of 3.1 ± 0.37 nm and a density of approximately 2.15×10^{11} cm^{-2} . The results revealed that most of the nc-Si fall in one of the

two main particle groups with diameter size of 2.7 ± 0.32 and 3.3 ± 0.39 nm, which is in accordance with the nc-Si size calculated using the PL peaks of Fig. 2(a) and the quantum confinement model. An EDX measure was performed to one of the three nc-Si that are shown in the bottom of Fig. 3(b), in order to verify the composition of the nanocrystals that were formed during the growing process. The results show the following elemental concentrations: 95% Si, 2% O and 3% Cu. It has been observed [9] that the nc-Si size can be controlled by changing the NH_3 flow concentration during the growing process. Crystallographic planes of a nc-Si as well as the orientation of the crystalline planes given by the Fourier Transform (FT) of our nanocrystal image are shown in Fig. 3(c). The results obtained from the EDX analysis as well as the FT make us assure that the nc-Si obtained by the RPECVD growing technique are crystalline and composed by silicon.

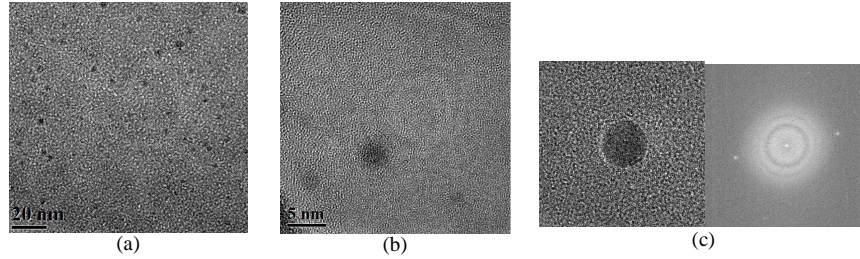


Fig. 3. HRTEM images of nc-Si embedded in a silicon nitride matrix.

In order to study the nanosecond nonlinear response in our sample, we measured its optical ablation threshold for avoiding optical damage, and we obtained $42 \text{ J/cm}^2 \pm 10\%$. We acquired the self-diffracted intensity of the wave \vec{E}_3 in our experiment, and an error bar of $\pm 10\%$ was estimated for our intensity data. In this case, the polarization of the wave \vec{E}_1 was fixed, and the polarization of the wave \vec{E}_2 was rotated by the half-wave plate. We calculate the self-diffraction efficiency η , as the ratio between the intensities of the first and the zero order of diffraction of the incident beam. We first compare the numerical simulations calculated from Eqs. (5)-(8) with our data obtained from the single pulses experiments ($< 1\text{Hz}$) and showed in Fig. 4(a). In this particular case we consider the initial point with $\Delta T = 0$. We then adjust the values of β and the parameters A and B . We obtain the relation between the parameters A and B in Eqs. (3) and (4), resulting $B/A = 1$, which allows us to identify that the electronic polarization is present as a mechanism responsible for the observed nonlinear refraction in our sample [4]. From the data shown in Fig. 4(a), a nonzero change in the self-diffraction intensity can be observed when an increment on the repetition rate of the pulses is made (1Hz and 10Hz). This indicates that a thermal effect is present. Using Eq. (1) with $\kappa = 16.33 \text{ W/m}^\circ\text{K}$, $\rho = 0.01908 \text{ mol/cm}^3$, and $C = 30.25 \text{ J/mol}^\circ\text{K}$ in our sample, we calculate that after 0.1s a single pulse of our laser gives a change in temperature $\Delta T = 0.01^\circ\text{K}$ in our self-diffraction experiment. In order to discern the real and imaginary parts of $\chi^{(3)}$, we consider that thermal relaxation occurs between pulses when we have a repetition rate $< 0.1\text{Hz}$. Thus we calculate the value of dn/dT in Eqs (5)-(8) using the pulses 10Hz; in this particular case we expect the same electronic contribution to the nonlinear effect, and an additional increase in the thermal effect caused by an increment of the energy deposited per unit of time, as a consequence the change in the product of dn/dT and ΔT . We find that $dn/dT = 1 \times 10^{-4} \text{ }^\circ\text{C}^{-1}$ and $\beta = 1 \times 10^{-9} \text{ m/W}$. Finally we calculate that the response associated with the thermal and the electronic nonlinearity in our sample is $|\chi_{1111}^{(3)}| = 3.3 \times 10^{-10} \text{ esu}$, and $n_2 = 2.7 \times 10^{-16} \text{ m}^2/\text{W}$. In Fig. 4(a) we show our experimental data and numerical results, with the best fit of the parameters calculated. We used single pulses of 532nm for evaluating comparatively the change in the refractive index in our sample when its temperature is elevated homogeneously 2°C from 19°C ,

then we obtained a $dn/dT = 9 \times 10^{-5} \text{ } ^\circ\text{C}^{-1} \pm 25\%$. This result is consistent with our self-diffraction results.

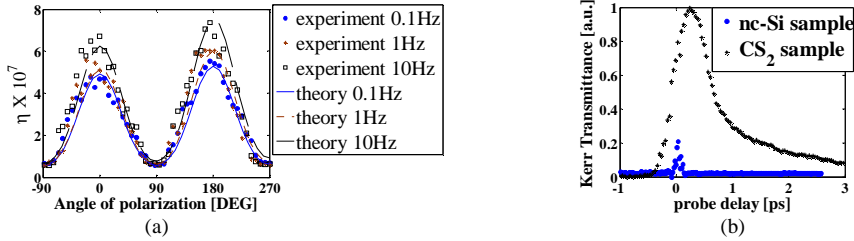


Fig. 4. (a). Self-diffraction intensity obtained at different repetition rate of ns pulses, (b) Kerr Transmittance versus probe delay in the fs experiment.

For short (ps) and ultrashort (fs) pulses, a high peak irradiance can be achieved while minimizing the thermal load to the sample. For this reason we used fs pulses at 830 nm to determine the electronic nonlinearity in this regime, without the concurrent effect of a thermal process. Figure 4(b) shows the signal obtained using the optical Kerr gate technique, with the experimental set up illustrated in Fig. 1(b), for a sample of CS₂ contained in a 1 mm thick quartz cell and our nc-Si sample. We conducted standard pump-probe experiments in order to quantify the nonlinear absorption on the sample. From the results, we did not observe TPA even with the highest energies (3.4nJ) available from our laser system. We used Eqs. (5)-(8)

for calculating the nonlinear response and we obtained a $|\chi_{1111}^{(3)}| = 9.5 \times 10^{-11}$ esu for the fs

regime. In comparison to the ns regime, we associated the decrement of $|\chi_{1111}^{(3)}|$ to the absence of the contribution of the thermal effect to the third order nonlinearity in the purely electronic femtosecond response. The nonlinear parameters of our sample are very close to the reported data for nc-Si-SiO₂[10], and pure silicon [11]; even though different sign and magnitudes has been reported in literature[12]. The nonlinear response that we obtained from silicon nitride films without any nc-Si is at least one order of magnitude weaker than the response from our sample with nc-Si. In comparison with our sample, pure silicon presents lower optical damage threshold in at least six times of magnitude [13]; furthermore, nanostructured materials in silica with similar magnitude of nonlinear response also exhibit much lower optical damage threshold [14] in comparison to the value presented by our sample. We emphasize that we can manipulate the nonlinear response of our sample by means of its physical mechanisms of nonlinearity, specially the contribution of thermo-optic properties.

5. Conclusion

We present a study of the third order nonlinear optical response in a silicon nitride sample containing nc-Si. We consider that the intensities obtained in a vectorial self-diffraction experiment are function of the physical mechanisms of nonlinearity of index in the sample, and from varying the repetition rate of nanosecond pulses we showed the possibility for measuring and identifying the thermal and the electronic mechanisms of nonlinearity for our sample. For studying the purely electronic response, far from resonance of our sample, we used femtosecond pulses at 830nm in a Kerr gate experiment. We associated the differences in the $|\chi_{1111}^{(3)}|$ values for our nanosecond and femtosecond results to the different contributions of the physical mechanisms of nonlinearity involved in the interactions. It is interesting to consider that a high optical damage threshold was observed and the significant thermo optic coefficient makes our sample a promising material for all-optical filtering applications based on thermal and optical Kerr effects.

Acknowledgments

The authors wish to acknowledge the technical assistance of K. López, F. J. Jaimes, L. Rendón and D. Quiterio-Vargas. This work has been partially supported by DGAPA-UNAM under project PAPIIT-IN101908.